

# The roles of nucleon resonances in $\Lambda(1520)$ photoproduction off proton

Jun He<sup>1,2,\*</sup> and Xu-Rong Chen<sup>1,2</sup>

<sup>1</sup> Institute of Modern Physics, Chinese Academy of Sciences, Lanzhou 730000, China

<sup>2</sup> Research Center for Hadron and CSR Physics, Institute of Modern Physics of CAS and Lanzhou University, Lanzhou 730000, China

(Dated: September 1, 2020)

In this work the roles of the nucleon resonances in the  $\Lambda(1520)$  photoproduction off proton target are investigated within the effective Lagrangian method. Besides the Born terms, including contact term,  $s$ -,  $u$ - and  $K$  exchanged  $t$ -channels, vector meson  $K^*$  exchanged  $t$ -channel is considered in our investigation, which is negligible at low energy and important at high energy. The important nucleon resonances predicted by the constituent quark model (CQM) are considered and the results are found well comparable with the experimental data. Besides the dominant  $D_{13}(2080)$ , the resonance  $[\frac{5}{2}^-]_2(2080)$  predicted by the CQM is found important to reproduce the experimental data. Other nucleon resonances are found to give small contributions in the channel considered in this work. With all important nucleon resonances predicted by CQM, the prediction of the differential cross section at the energy up to 5.5 GeV are presented also, which can be checked by the future CLAS experimental data.

PACS numbers: 14.20.GK, 13.75.Cs, 13.60.Rj

## I. INTRODUCTION

The study of nucleon resonance is an interesting area in hadron physics. As of now, the nucleon resonances around 2.1 GeV are still in confusion. The CQM predicted about two dozens of the nucleon resonances in this region, most of which are in  $n = 3$  shell. Only a few of them have been observed as shown in PDG with large uncertainties [1]. Among these nucleon resonances,  $D_{13}(2080)$  attracts much attentions due to its importance found in many channels, such as  $\gamma p \rightarrow K^* \Lambda$  [2] and  $\phi$  photoproduction [3]. In the analyses of the data for  $\gamma p \rightarrow \eta' p$  by Zhang *et al.* and Nakayama *et al.* the contribution of  $D_{13}(2080)$  is also found important to reproduce the experimental data [4, 5]. However, in the recent work by Zhong *et al.* [6], the bump-like structure around  $W = 2.1$  GeV is from the contribution of a  $n = 3$  shell resonance  $D_{15}(2080)$  instead of  $D_{13}(2080)$ . In Ref. [7], the  $\eta$  photoproduction off the proton is studied in a chiral quark model, a  $D_{15}$  resonance instead of  $D_{13}$  state with mass about 2090 MeV is also suggested to reproduce the experimental data. Hence, more efforts should be paid to figure out the nucleon resonances around 2.1 GeV.

After many years of efforts, a mount of experimental data for the nucleon resonances below 2 GeV have been accumulated while these above 2 GeV are still scarce. Due to the high threshold of  $\Lambda(1520)$  production, about 2 GeV, it is appropriate to enrich the acknowledge of the nucleon resonances especially the ones with the mass larger than 2 GeV. There exist some old experiments for kaon photoproduction off the nucleon with  $\Lambda(1520)$ . In the last seventies, SLAC [8] used a 11 GeV photon beam on hydrogen to study the inclusive reaction  $\gamma p \rightarrow K^+ Y$ , where  $Y$  represents a produced hyperon. The LAMP2 collaboration at Daresbury [9] studied the exclusive reaction  $\gamma p \rightarrow K^+ \Lambda^*$  with  $\Lambda^* \rightarrow p K^-$  at photon energies ranging from 2.8 GeV to 4.8 GeV. In the recent years, excited by the claimed finding of pentaquark  $\Theta$  with mass about

1.540 GeV reported by LEPS collaboration in 2003 [10], many experiments are performed in the  $\Lambda(1520)$  energy region due to the close mass of  $\Lambda(1520)$  and  $\Theta$ . Though the pentaquark is doubtful based on the later more precise experiments, many experimental data about  $\Lambda(1520)$  photoproduction are accumulated, which provides opportunity to understand the reaction mechanism of  $\Lambda(1520)$  photoproduction off nucleon and the possible nucleon resonances in this reaction.

The LEPS experiment (labeled as LEPS09 in this work) in the Spring-8 measured the  $\Lambda(1520)$  photoproduction with liquid hydrogen and deuterium targets at photon energies below 2.4 GeV [11]. A large asymmetry of the production cross sections in the proton and neutron channels was observed at backward  $K^{+0}$  angles. It supports the conclusion by Nam *et al.* [12] that the contact term, with  $t$ -channel  $K$  exchange under gauge invariance, plays the most important role in the  $\Lambda(1520)$  photoproduction and the contribution from resonances  $D_{13}(2080)$  is small and negligible. Differential cross sections and photon-beam asymmetries for the  $\gamma p \rightarrow K^+ \Lambda(1520)$  reaction have been measured by LEPS Collaboration (labeled as LEPS10) with linearly polarized photon beams at energies from the threshold to 2.4 GeV at  $0.6 < \cos \theta_{CM}^K < 1$  [13]. A new bump structure was found at  $W \approx 2.1$  GeV in the cross sections. Xie *et al.* suggested the bump structure could be reproduced by including the resonance  $D_{13}(2080)$  [14]. For the polarized symmetry, the theoretical result by Xie *et al.* seems to have an inverse sign compared with the LEPS10 data. The model by Nam *et al.* also give near zero polarized asymmetry [13].

In Refs. [15, 16], the electromagnetic and strong decays were studied in the CQM, with which the contributions of the nucleon resonances in the photoproductions can be calculated in Ref. [17]. In this work we will investigate the  $\Lambda(1520)$  photoproduction within the effective Lagrangian method, with the nucleon resonances included according to the CQM prediction, to find the roles of nucleon resonances, especially the  $D_{13}$  and  $D_{15}$  states around 2.1 GeV, played in the reaction mechanism.

---

\*Electronic address: junhe@impcas.ac.cn

This paper is organized as follows. After introduction, we will present the effective Lagrangian used in this work and the amplitudes based on the effective Lagrangian. The differential cross section at the low energy and the prediction at high energy will be given in section III. Finally the paper ends with a brief summary.

## II. FORMALISM

The mechanism for the  $\Lambda(1520)$  photoproduction off nucleon with  $K$  is figured as the following diagrams in Fig. 1. In this work, due to the small contribution from the  $u$ -channel

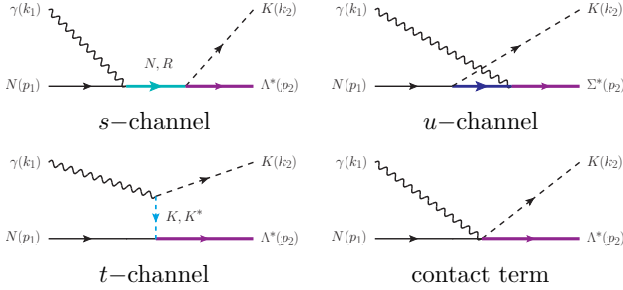


FIG. 1: (Color online) The diagrams for the  $s$ -,  $u$ -,  $t$ -channel and contact term.

as shown in the literatures [12, 14, 18] it is not considered in this work. Besides the Born terms, including  $s$ -,  $K$  exchanged  $t$ -channels and contact term, the contributions from the  $K^*$  exchanged  $t$ - and resonance ( $R$ ) intermediate  $s$ -channels are considered in the current work.

### A. Born terms

The Lagrangians used in the Born terms are given below [12, 14],

$$\begin{aligned}\mathcal{L}_{\gamma KK} &= ieQ_K \left[ (\partial^\mu K^\dagger) K - (\partial^\mu K) K^\dagger \right] A_\mu, \\ \mathcal{L}_{\gamma NN} &= -e\bar{N} \left[ Q_N \not{A} - \frac{\kappa_N}{4M_N} \sigma^{\mu\nu} F^{\mu\nu} \right] N, \\ \mathcal{L}_{KN\Lambda^*} &= \frac{g_{KN\Lambda^*}}{M_{\Lambda^*}} \bar{\Lambda}^{*\mu} \partial_\mu K \gamma_5 N + \text{h.c.}, \\ \mathcal{L}_{\gamma KN\Lambda^*} &= -\frac{ieQ_N g_{KN\Lambda^*}}{M_{\Lambda^*}} \bar{\Lambda}^{*\mu} A_\mu K \gamma_5 N + \text{h.c.},\end{aligned}\quad (1)$$

where  $F^{\mu\nu} = \partial^\mu A^\nu - \partial^\nu A^\mu$  with  $A^\mu$ ,  $N$ ,  $K$ ,  $\Lambda^*$  are the photon, nucleon, kaon and  $\Lambda^*(1520)$  fields. Here  $Q_h$  is the charge in the unit of  $e = \sqrt{4\pi\alpha}$ . The anomalous magnetic momentum  $\kappa = 1.79$  for proton. The coupling constant  $g_{KN\Lambda^*} = 10.5$  obtained from the decay width of  $\Lambda^* \rightarrow NK$  in Particle Data Group (PDG) [1].

For  $K^*$  exchange  $t$ -channel, we need the following Lagrangians,

$$\mathcal{L}_{\gamma KK^*} = g_{\gamma KK^*} \epsilon_{\mu\nu\sigma\rho} (\partial^\mu A^\nu) (\partial^\sigma K^{*\rho}) K + \text{h.c.}, \quad (2)$$

$$\mathcal{L}_{K^*N\Lambda^*} = -\frac{ig_{K^*N\Lambda^*}}{m_{K^*}} \bar{\Lambda}^{*\mu} \gamma^\nu F_{\mu\nu} N + \text{h.c.}, \quad (3)$$

with the coupling constant  $g_{\gamma K^* K^*} = 0.254 \text{ GeV}^{-1}$  extracted from decay width in PDG [1]. A Reggeized treatment will be applied to  $t$ -channel. As discussion in Ref [19], the coupling constant for the Reggeized treatment can be different from the one in the effective Lagrangian approach. Here we do not adopt the value about 1 determined by  $SU(6)$  model [20], but the larger one, about 10, by quark model [20] and phenomenological fitting of Nam *et al.* [18] and Totiv *et al.* [21].

The scattering amplitude for the photoproduction can be written as follow:

$$-i\mathcal{T}_{\lambda_{\Lambda^*}, \lambda_\gamma, \lambda_N} = \bar{u}_\mu(p_2, \lambda_{\Lambda^*}) A^{\mu\nu} u(p_1, \lambda_N) \epsilon_\nu(k_1, \lambda_\gamma) \quad (4)$$

where  $\epsilon_\nu$ ,  $u_1$ , and  $u_2^\mu$  denote the photon polarization vector, nucleon spinor, and RS vector-spinor, respectively.  $\lambda_{\Lambda^*}$ ,  $\lambda_\gamma$  and  $\lambda_N$  are the helicities for  $\Lambda(1520)$ , photon and nucleon.

The amplitudes for Born  $s$ -,  $t$ -channels and contact term are

$$\begin{aligned}A_s^{\mu\nu} &= -\frac{eg_{KN\Lambda^*}}{m_K} \frac{1}{s - M_N^2} k_2^\mu \gamma_5 \\ &\quad \left[ Q_N ((p_1 + M_N) F_c + k_1 F_s) \gamma^\nu \right. \\ &\quad \left. + \frac{\kappa_N}{2M_N} (k_1 + p_1 + M_N) \gamma^\nu k_1 F_s \right],\end{aligned}\quad (5)$$

$$A_t^{\mu\nu} = \frac{eQ_K g_{KN\Lambda^*} F_c}{m_K} \frac{1}{t - m_K^2} q^\mu k_2^\nu \gamma_5, \quad (6)$$

$$A_{\text{cont.}}^{\mu\nu} = \frac{eQ_N g_{KN\Lambda^*} F_c}{m_K} g^{\mu\nu} \gamma_5, \quad (7)$$

where  $s$ ,  $t$ , and  $u$  indicate the Mandelstam variables.

The amplitude for  $K^*$  exchange is

$$\begin{aligned}A_t^{K^*} &= \frac{ig_{\gamma KK^*} g_{K^*N\Lambda^*} F_V}{m_{K^*}} \frac{1}{t - m_{K^*}^2} (\epsilon_{\sigma\rho\xi\nu} k_1^\rho k_2^\xi) \\ &\quad \gamma_\nu \left[ (k_1^\mu - k_2^\mu) g^{\nu\sigma} + (k_1^\nu - k_2^\nu) g^{\mu\sigma} \right].\end{aligned}\quad (8)$$

The form factors are introduced in the same form,

$$F_i = \left( \frac{n\Lambda_i^4}{n\Lambda_i^4 + (q_i^2 - M_i^2)^2} \right)^n, \quad (9)$$

$$F_c = F_s + F_t - F_s F_t \quad (10)$$

where  $i$  means  $s$ ,  $t$ ,  $V$  and  $R$  corresponding to  $s$ -,  $t$ -channel, vector exchange  $t$ -channel and resonance intermediate  $s$ -channel.

To describe the behaviour at the high photon energy, we introduce the pseudoscalar and vector strange-meson Regge trajectories following [21–23]:

$$\begin{aligned}\frac{1}{t - m_K^2} &\rightarrow \mathcal{D}_K = \left( \frac{s}{s_0} \right)^{\alpha_K} \frac{\pi \alpha'_K}{\Gamma(1 + \alpha_K) \sin(\pi \alpha_K)}, \\ \frac{1}{t - m_{K^*}^2} &\rightarrow \mathcal{D}_{K^*} = \left( \frac{s}{s_0} \right)^{\alpha_{K^*} - 1} \frac{\pi \alpha'_{K^*}}{\Gamma(\alpha_{K^*}) \sin(\pi \alpha_{K^*})},\end{aligned}\quad (11)$$

where  $\alpha'_{K,K^*}$  indicates the slope of the trajectory.  $\alpha_{K,K^*}$  is the linear trajectory of the meson for even or odd spin, which is a function of  $t$  assigned as follows,

$$\alpha_K = 0.70 \text{ GeV}^{-2}(t - m_K^2), \quad (12)$$

$$\alpha_{K^*} = 1 + 0.85 \text{ GeV}^{-2}(t - m_{K^*}^2). \quad (13)$$

To restore the gauge invariance, we redefine the relevant amplitudes as follow [12],

$$\begin{aligned} & i\mathcal{M}_K + i\mathcal{M}_s^E + i\mathcal{M}_c \\ \rightarrow & i\mathcal{M}_K^{\text{Regge}} + (i\mathcal{M}_s^E + i\mathcal{M}_c)(t - m_K^2)\mathcal{D}_K \end{aligned} \quad (14)$$

The Reggeized treatment should work completely at high photon energies and interpolate smoothly to low photon energy. It have been considered by Toki *et al.* [19] and Nam *et al.* [12] by introducing a weighting function. Here we adopt the treatment by Nam *et al.*,

$$F_{c,v} \rightarrow \bar{F}_{c,v} \equiv \left[ (t - m_{K,K^*}^2)\mathcal{D}_{K,K^*} \right] \mathcal{R} + F_{c,v}(1 - \mathcal{R}), \quad (15)$$

where  $\mathcal{R} = \mathcal{R}_s \mathcal{R}_t$  with

$$\begin{aligned} \mathcal{R}_s &= \frac{1}{2} \left[ 1 + \tanh \left( \frac{s - s_{\text{Regge}}}{s_0} \right) \right], \\ \mathcal{R}_t &= 1 - \frac{1}{2} \left[ 1 + \tanh \left( \frac{|t| - t_{\text{Regge}}}{t_0} \right) \right]. \end{aligned} \quad (16)$$

In this work the values of the four parameters for the reggeized treatment are chosen as Nam. *et al.* as presented in Table I.

TABLE I: parameters for the reggeized treatment with unit  $\text{GeV}^2$ .

$s_{\text{Reg}} = 3$	$t_{\text{Reg}} = 0.1$	$s_0 = 1$	$t_0 = 0.08$
----------------------	------------------------	-----------	--------------

## B. Nucleon resonances

In Ref. [14], the  $D_{13}(2080)$  is considered to reproduce the bump structure near 2.1 GeV. In this work all resonances predicted by CQM will be considered. The Lagrangians for the resonances with arbitrary half-integer spin are [24–26]

$$\mathcal{L}_{\gamma NR(\frac{1}{2}^\pm)} = \frac{ef_2}{2M_N} \bar{N} \Gamma^{(\mp)} \sigma_{\mu\nu} F^{\mu\nu} R + \text{h.c.}, \quad (17)$$

$$\begin{aligned} \mathcal{L}_{\gamma NR(J^\pm)} &= \frac{-i^n f_1}{(2m_N)^n} \bar{B}^* \gamma_\nu \partial_{\mu_2} \dots \partial_{\mu_n} F_{\mu_1\nu} \Gamma^{\pm(-1)^{n+1}} R^{\mu_1\mu_2\dots\mu_n} \\ &+ \frac{i^{n+1} f_2}{(2m_N)^{n+1}} \partial_\nu \bar{B}^* \partial_{\mu_2} \dots \partial_{\mu_n} F_{\mu_1\nu} \Gamma^{\pm(-1)^{n+1}} R^{\mu_1\mu_2\dots\mu_n} \\ &+ \text{h.c.}, \end{aligned} \quad (18)$$

where  $R_{\mu_1\dots\mu_n}$  is the field for the resonance with spin  $J = n + 1/2$ , and

$$\Gamma^{(\pm)} = (i\gamma_5, 1) \quad (19)$$

for the different parity of resonance. The Lagrangians are also adopted by the previous works on the nucleon resonances with spins 3/2 or 5/2 [12, 14, 17, 27].

The Lagrangian for the strong decay can be written as

$$\mathcal{L}_{RK\Lambda^*} = \frac{ig_2}{2m_K} \partial_\mu K \bar{\Lambda}_\mu^* \Gamma^{(\pm)} R + \text{h.c.}, \quad (20)$$

$$\begin{aligned} \mathcal{L}_{RK\Lambda^*} &= \frac{i^{2-n} g_1}{m_P^n} \bar{B}_{\mu_1}^* \gamma_\nu \partial_\nu \partial_{\mu_2} \dots \partial_{\mu_n} P \Gamma^{\pm(-1)^n} R^{\mu_1\mu_2\dots\mu_n} \\ &+ \frac{i^{1-n} g_2}{m_P^{n+1}} \bar{B}_\alpha^* \partial_\alpha \partial_{\mu_1} \partial_{\mu_2} \dots \partial_{\mu_n} P \Gamma^{\pm(-1)^n} R^{\beta\mu_1\mu_2\dots\mu_n} \\ &+ \text{h.c.} \end{aligned} \quad (21)$$

The corresponding propagator for the arbitrary half-inter spin can be found in Appendix A.

In this work the coupling constants  $f_1$ ,  $f_2$ ,  $g_1$  and  $g_2$  will be determined by the radiative and strong decays of the nucleon resonances. For a  $j = \frac{1}{2}$  resonance, the magnitudes of the coupling constants  $f_1$  and  $h_1$  can be determined by the radiative and strong decay widths. However, for nucleon resonances with high spin  $j \geq \frac{3}{2}$ , the decay widths are not enough to determine coupling constants,  $f_1$  and  $f_2$  for radiative decay or  $h_1$  and  $h_2$  for strong decay [17]. Therefore, we need to know the decay amplitudes to determine the coupling constants uniquely.

For the radiative decay, the helicity amplitudes are important physical quantities and can be extracted from the experiment data of photoproduction. The definition of the helicity amplitude is as below,

$$A_\lambda = \frac{1}{\sqrt{2|\mathbf{k}|}} \langle \gamma(\mathbf{k}, 1) N(-\mathbf{k}, \lambda - 1) | -iH_\gamma | R(\mathbf{0}, \lambda) \rangle \quad (22)$$

where  $|\mathbf{k}| = (M_R^2 - M_N^2)/(2M_R)$ ,  $\mathbf{k}$  is the momentum of photon in the center of mass system of the decaying nucleon resonance  $R$ , the  $\lambda = 1/2$  or  $3/2$  is the helicity. Since there are two amplitudes  $A_{1/2}$  and  $A_{3/2}$  for the resonances with  $J > 1/2$ , the coupling constants  $f_1$  and  $f_2$  in  $\mathcal{L}_{RN\gamma}$  can be extracted from the helicity amplitudes of the resonance  $R$ .

The coupling constants  $g_1$  and  $g_2$  can be calculated analogously by the following relation about the decay amplitude,

$$\begin{aligned} & \langle K(q) \Lambda^*(-q, m_f) | -i\mathcal{H}_{\text{int}} | R(\mathbf{0}, m_j) \rangle \\ &= 4\pi M_R \sqrt{\frac{2}{q}} \sum_{\ell, m_\ell} \langle \ell m_\ell \frac{3}{2} m_f | J m_j \rangle Y_{\ell m_\ell}(\hat{q}) G(\ell), \end{aligned} \quad (23)$$

where  $\langle \ell m_\ell \frac{3}{2} m_f | J m_j \rangle$ ,  $Y_{\ell m_\ell}(\hat{q})$  and  $G(\ell)$  are Clebsch-Gordan coefficient, the spherical harmonics function and the partial wave decay amplitude, respectively. The explicit is presented in Appendix B.

## III. RESULTS

With the Lagrangians presented in the previous section, the  $\Lambda(1520)$  photoproduction can be studied. With the contributions from nucleon resonances determined by the decay amplitudes, we will determine the parameters used in our model

first. Then the observables, such as differential cross section, will be calculated and compared with experiment.

### A. Contributions from nucleon resonances

The different cross section have been measured by LEPS09 and LEPS10 experiments. As found by Nam *et al.* and Xie *et al.* [12, 14], the most important contribution at the low energy for the differential cross section is from the contact term. The bump structure are from  $D_{13}(2080)$  suggested by Xie *et al.* by fitting the LEPS10 data. In this work we will use the helicity amplitudes  $A_\lambda$  and the partial wave decay amplitudes  $G(\ell)$  to describe the decays of the resonances. In experiment, the helicity amplitudes for the nucleon resonances with smaller mass are determined well while the ones for the resonances with larger mass especially the resonances with the mass larger than 2 GeV, which are considered in this work, are still not well determined and can not be compared well with the theoretical predictions.

In this work we will adopt the values obtained in the typical CQM by Capstick and Reborts [15, 16] as input. In their works the partial wave decay amplitudes are also provided. The nucleon resonances considered in the calculation are listed in Table II. The threshold of  $\gamma p \rightarrow K\Lambda(1520)$  is about 2.01 GeV, so only the nucleon resonances above 2.01 GeV are included in the calculation. In the works by Capstick [15, 16], about two dozens of nucleon resonances with spins up to 15/2 are calculated. In the current work, to simplify the claculation only the nucleon resonances with large radiative decay and strong decay to  $\Lambda(1520)K$  are used in the calculation of  $\Lambda(1520)$  photoproduction, which is reasonable in physics also.

For the masses of the nucleon resonances, the suggested values provided by PDG [1] are preferred and for the resonances not listed in PDG, the prediction by CQM will be adopted. Due to the dominance of  $D_{13}(2080)$  in the current channel, we adopt the mass suggested by Xie *et al.* [14], 2150 MeV, which is a little larger than the suggested value by PDG, 2080 MeV. In order to prevent the proliferation of the free parameters, the decay widths for all nucleon resonances are set to 200 MeV. Regarding the cut-offs for the nucleon resonances, the typical value  $\Lambda_R = 1$  GeV with  $n = 1$  is used. Therefore, the contributions from the nucleon resonances are fixed because the helicity amplitudes and partial wave decay amplitudes predicted by the CQM are adopted in the calculation to determine the coupling constants.

### B. Determination of model parameters

The contributions from the Born terms are very important as shown in the previous works. The magnitudes of contributions from contact term,  $u$ -,  $s$ - and  $K$  exchanges  $t$ - channels are only depended on the coupling constant  $g_{KN\Lambda^*}$ , which is determined by experimental decay width of  $\Lambda^* \rightarrow NK$ , and the cut off  $\Lambda$ . To reproduce the LEPS10 data, a cut-off

$\Lambda = 0.6$  GeV and  $n = 1$  should be used. With this setting, the  $s$ - channel contribution can be found very small.

Now we turn to the contribution of vector meson  $K^*$ -exchange. We consider the differential cross section at 11 GeV by SLAC at 11 GeV, where the contributions from contact term and  $t$ - channel should be dominant, which is confirmed by the results shown in Fig. 2.

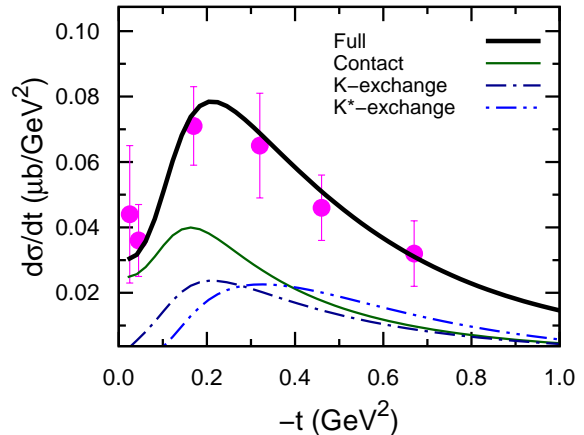


FIG. 2: (Color online) The differential cross section  $d\sigma/dt$  at 11 GeV and compared with the data by SLAC [8]. The thick full line is for the result in full model. The full, Dash-dotted and Dash-dot-dotted lines are for the contact term,  $K$ -exchange channel and  $K^*$ -exchange channel.

One can find at 11 GeV, the contribution from contact terms is still most important while the contribution from the  $K$ -exchanged  $t$ - channel becomes more important compared with that at the low energy. However, it is still not enough to reproduce the experimental data by including only the contributions from contact term and  $K$ -exchanged  $t$ - channel. In the work by Nam *et al.* [12] the differential cross section can be reproduced due to a larger cut-off  $\Lambda = 0.675$  GeV adopted. However, with such value of  $\Lambda$ , the differential cross section at low energy can not be well reproduced. The parameters for the Reggeized treatment,  $s_{0,Reg}$ ,  $t_{0,Reg}$  in Table I, are varied and it is found impossible to compensate the deficiency. Here we include the contribution of vector meson  $K^*$  exchange. With cutoff  $\Lambda_V = 0.8$  GeV and  $n = 2$ , the differential cross section by the SLAC experiment is well reproduced as shown in Fig. 2. In the figure one can find the contribution from vector meson  $K^*$ - exchange is comparable with the one from pseudoscalar meson  $K$ - exchange.

The determined cutoffs and the coupling constants for Born terms and the  $K^*$ -exchange are collected in Table III.

### C. Differential cross section

With the parameters determined and the amplitudes presented in Table II, the theoretical results of differential cross section at the low energy are presented in Fig. 3 and compared with the LEPS10 experiment. As shown in the figure,

TABLE II: The nucleon resonances considered. The mass  $m_R$ , helicity amplitudes  $A_\lambda$  and partial wave decay amplitudes  $G(\ell)$  are in the unit of MeV,  $10^{-3}/\sqrt{\text{GeV}}$  and  $\sqrt{\text{MeV}}$ , respectively. The last column is for  $\chi^2$  after turning off the corresponding nucleon resonance with  $\chi^2 = 1.38$  in full model.

State	PDG	$M_R$	$A_{1/2}^p$	$A_{3/2}^p$	$G(\ell_1)$	$G(\ell_2)$	$\sqrt{\Gamma_{\Lambda(1520)K}}$	$\chi^2$
$[N_{\frac{1}{2}}^-]_3(1945)$	$N(2090)S_{11}^*$	2090	12		$6.4^{+5.7}_{-6.4}$		$6.4^{+5.7}_{-6.4}$	1.89
$[N_{\frac{3}{2}}^-]_3(1960)$	$N(2080)D_{13}^{**}$	2150	36	-43	$-2.6^{+2.6}_{-2.8}$	$-0.2^{+0.2}_{-1.3}$	$2.6^{+2.9}_{-2.6}$	12.42
$[N_{\frac{5}{2}}^-]_2(2080)$		2080	-3	-14	$-4.7^{+4.7}_{-1.2}$	$-0.3^{+0.3}_{-0.8}$	$4.7^{+1.3}_{-4.7}$	4.01
$[N_{\frac{5}{2}}^-]_3(2095)$	$N(2200)D_{15}^{**}$	2200	-2	-6	$-2.4^{+2.4}_{-2.0}$	$-0.1^{+0.1}_{-0.3}$	$2.4^{+2.0}_{-2.4}$	1.59
$[N_{\frac{7}{2}}^-]_1(2090)$	$N(2190)G_{17}^{****}$	2190	-34	28	$-0.5^{+0.4}_{-0.6}$	$0.0^{+0.0}_{-0.0}$	$0.5^{+0.6}_{-0.4}$	1.48
$[N_{\frac{7}{2}}^+]_2(2390)$		2390	-14	-11	$3.1^{+0.8}_{-1.2}$	$0.3^{+0.3}_{-0.2}$	$3.1^{+0.8}_{-1.2}$	1.79

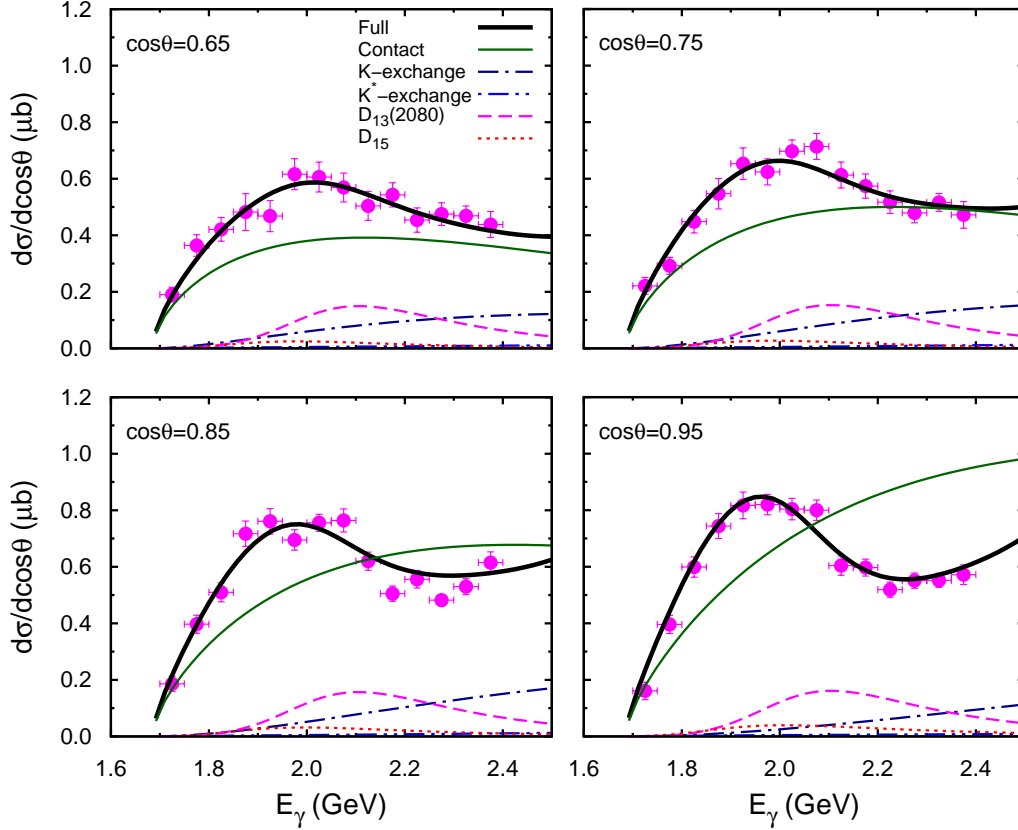


FIG. 3: (Color online) The differential cross section  $d\sigma/d\cos\theta$  at low photon energy and compared with the data by LEPS10. The thick full line is for the results in full model. The full, Dash-dotted and Dash-dot-dotted lines are for contact term,  $K$ -exchange channel and  $K^*$ -exchange channel. The dashed (dotted) line is for nucleon resonance  $D_{13}(2080)$  ( $D_{15}$ ).

TABLE III: The coupling constants for the  $K$  and  $K^*$  exchanged channel and cut-offs in the unit of GeV.

$g_{\gamma K^* K^{*\mp}}$	0.254	$g_{KN\Lambda^*}$	10.5	$\bar{g}_{K^* N\Lambda^*}$	10
$\Lambda$	0.6	$\Lambda_V$	0.8	$\Lambda_R$	1

the experimental data are well reproduced in our model. The dominant contributions are from Born terms where the contact term play most important role. At the low energy the  $K$

exchange contribution is smaller but visible while the vector meson  $K^*$  exchanged contribution is negligible.

To find the importance of each nucleon resonance, the  $\chi^2$  for the differential cross section from threshold to 2.5 GeV by LEPS10 experiment and these at 11 GeV by SLAC is calculated.  $\chi^2$  obtained in the current work is 1.38, which is a little larger than the 1.2 obtained by Xie *et al.* but close to 1.4 in their fitting with strong coupling constant as free parameters [14]. We would like to remind that in the current work both electromagnetic and strong coupling constants are determined from CQM predictions with the physics choice of the

mass and cut-off for the nucleon resonance.

To check the role of nucleon resonance played in  $\Lambda(1520)$  photoproduction, we list the  $\chi^2$  after truing off the corresponding nucleon resonance in Table II. Compared with the value  $\chi^2 = 1.38$  in the full model,  $\chi^2$  after turning off the  $D_{13}(2080)$  increases significantly to 12.42, which confirms the dominant role played by this resonance as suggested by Xie *et al.* [14]. Besides the dominant  $D_{13}(2080)$ , the contribution from a  $D_{15}$  resonances is also important. After turning off  $[\frac{5}{2}^-]_2(2080)$ , the  $\chi^2$  will increase to 4.01 due to the interference effect mainly. Simultaneously the  $[\frac{5}{2}^-]_3(2095)$  is found not important with  $\chi^2 = 1.59$  after being turned off. In PDG [1] a  $D_{15}$  state  $N(2200)$  is listed, which is assigned to the  $[\frac{5}{2}^-]_3(2095)$  in the CQM usually [15]. The predicted decay amplitudes in  $N\pi$  and  $\Lambda K$  channels for  $[\frac{5}{2}^-]_3(2095)$  are close to those for  $[\frac{5}{2}^-]_2(2080)$  [15]. To check whether the  $D_{15}$  state  $[\frac{5}{2}^-]_2(2080)$  instead of  $[\frac{5}{2}^-]_3(2095)$  is the observed resonance  $N(2200)$  listed in PDG, we vary the mass of  $[\frac{5}{2}^-]_2(2080)$  to 2.2 GeV and a  $\chi^2$  about 4 is found. It indicat that the experimental data require the mass of  $[\frac{5}{2}^-]_2(2080)$  should be about 2.08 GeV. Hence  $[\frac{5}{2}^-]_2(2080)$  should not be assigned to  $N(2200)$  due to the large mass discrepancy about 100 MeV.

To give a picture around the resonance poles, we calculate the  $d\sigma/d\cos\theta$  against  $\theta$  at 2.2 GeV and compared with LEPS09 data as shown in Fig. 4.

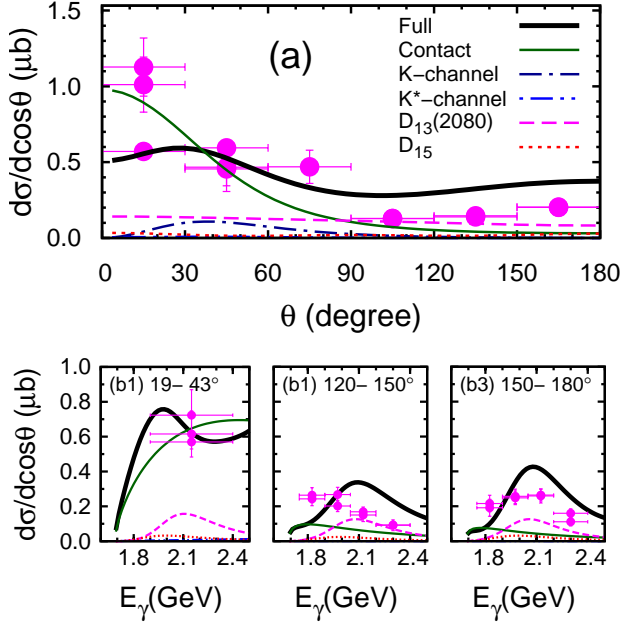


FIG. 4: (Color online) (a) The differential cross section  $d\sigma/d\cos\theta$  with the variation of  $\theta$  at photon energy 2.2 GeV compared with the data by LEPS09 at photon energy 1.9-2.4 Ge. (b1-b3) The differential cross section  $d\sigma/d\cos\theta$  with the variation of photon energy  $E_\gamma$ . Notation as in Fig. 3.

The experimental data are reproduced generally in our model. One can find the general shape for the differential cross section against  $\theta$  is mainly formed by the contact term

contribution. The slow increase in the backward is from the resonances contributions. For differential cross section with the variation of  $E_\gamma$ , the nucleon resonances give contributions larger than the contact term and are responsible to the bump at the backward angles.

#### D. Polarized asymmetry

The polarized asymmetry was measured in the LEPS10 experiment. Nearly zero polarized asymmetry was obtained in the model by Nam *et al.* [13]. In Ref. [14] the result suggested the sign should be reversed compared with the experiment. In this work, the similar result as Ref [14] is obtained as shown in Fig. 5. It suggests that further improvement may be needed based on the effective Lagrangian method, such as the lack of unitary, coupled-channel effects.

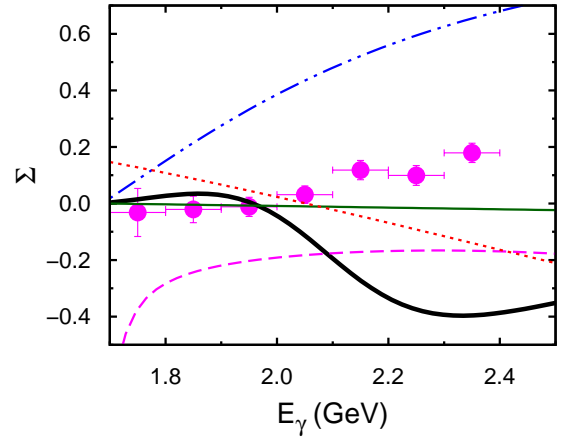


FIG. 5: (Color online) Polarization asymmetry and compared with LEPS10. Notation as in Fig. 3

#### E. Prediction of differential cross section at high energy

In the above sections, all parameters, such as cut-offs, are determined and the contributions from nucleon resonances are introduced by the CQM predictions. With these parameters the differential cross sections at energy below 2.5 GeV and at the energy 11 GeV have been reproduced well. Hence it is possible to give the prediction in the higher energy than 2.5 GeV. Recently CLAS collaboration reported that the  $\Lambda(1520)$  photoproduction was measured at the photon energy from 1.87 to 5.5 GeV and some preliminary results have been obtained in the  $eg3$  run [28]. The  $g_{11}$  experiment also run in this energy region. Therefore, it is meaningful to make predictions. The differential cross section  $d\sigma/d\theta$  predicted by the model obtained in this work are presented in Fig. 6.

The contributions from  $D_{13}(2080)$  and  $D_{15}(2080)$  are still most important as well as at the low energy. The  $[\frac{7}{2}^-]_2(2390)$  is small at high energy though it has higher mass. The contribution from the contact term plays most important role at the

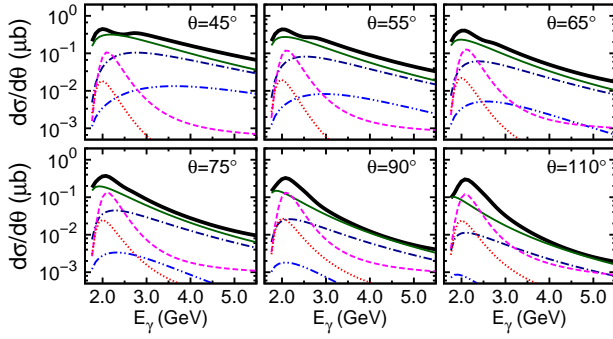


FIG. 6: (Color online) The differential cross section  $d\sigma/d\theta$  with the variation of photon energy  $E_\gamma$  predicted in this work. Notation as in Fig. 3

energy up to 5.5 GeV especially at the forward angles while the contributions from two resonances will decrease rapidly at the photon energy large than the energy point corresponding to the Breit-Wigner mass.

The dominance of contact contribution at the higher photon energy can be observed more obviously in the differential cross section  $d\sigma/dt$  as shown in Fig. 7.

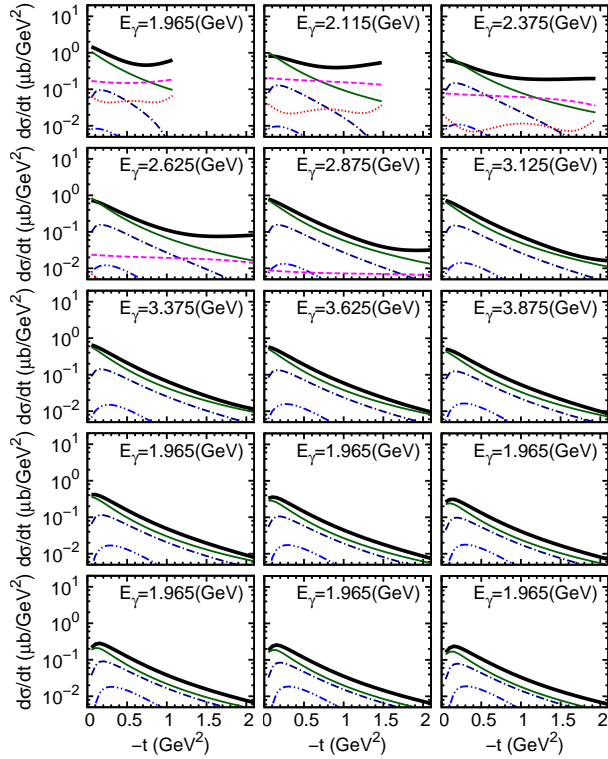


FIG. 7: (Color online) The differential cross section  $d\sigma/dt$  with variation of  $-t$  predicted in this work. Notation as in Fig. 3

One can find at high photon energy, the contact contribution is several times larger than the vector meson  $K^*$  exchange and the contributions from the resonances are negligible. The contributions from the nucleon resonances  $D_{13}(2080)$  and  $D_{15}$  are

important at low energy, and give a slow increase in the large  $|t|$  region.

## F. Total cross section

As of now, there only exist a few experimental data about the total cross section. The data by SAPHIR experiment are only at the low energy [29] while LAMP2 experiment gives some data at high energy [9]. In Fig. 8, we show the theoretical results in our model and compared with the experimental data.

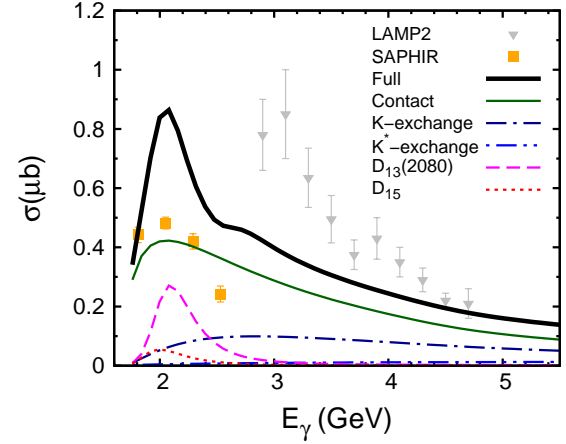


FIG. 8: (Color online) Total cross section  $\sigma$  with the variation of the energy of photon  $E_\gamma$ . Notations for the theoretical results as in Fig. 3. The data are from Refs. [9, 29].

As shown in the Fig. 8, though two sets of data do not have overlap in energy, it can be easily found that they are not consistent with each other. The old LAMP2 data are higher than the SAPHIR data systemically. Our result is just in the midst of two sets of data. As indicated in the differential cross section, the nucleon resonances  $D_{13}(2080)$  and  $D_{15}$  are responsible to the peak around 2.1 GeV.

## IV. SUMMERY

In this work we investigate the  $\Lambda(1520)$  photoproduction in the  $\gamma N \rightarrow K\Lambda(1520)$  reaction within the effective Lagrangian method. The contact term is dominant in the interaction mechanism and  $K$  exchanged  $t$ -channel are important except at the energy near the threshold. The  $K^*$ -exchange  $t$ -channel plays important role in the high energy at 11 GeV but is negligible at low energy.

The contributions of nucleon resonances are determined by the radiative and strong decay amplitudes predicted by the constituent quark model. The results shows that  $D_{13}(2080)$  is the most important nucleon resonance in  $\Lambda(1520)$  photoproduction and responsible to the bump structure in the LEPS10 experiment. A nucleon resonance  $[\frac{5}{2}^-]_2(2080)$  predicted by

CQM with mass about 2100 MeV, which can not be assigned as  $N(2200)$ , is also essential to reproduce the experimental data around 2.1 GeV. The contributions from other nucleon resonances are small even negligible.

With the contributions from Born terms and nucleon resonances, the experimental data about differential cross sections can be reproduced while there exists large discrepancy between experimental and theoretical results in polarized asymmetry, which suggests further improvement, such as including the coupled-channel effect, is required. The predictions about the differential cross section at energy  $1.75 \text{ GeV} < E_\gamma < 5.50 \text{ GeV}$  are presented, which can be checked by the future experimental data in the CLAS  $eg3$  and  $g11$  runs.

### Acknowledgement

This project is partly supported by the National Natural Science Foundation of China under Grants No. 10905077, No. 11035006.

### Appendix A: propagator

In this appendix, we will present the propagator of half-integral spin particle used in the current work, which is in the same theoretical frame of the Lagrangians in Eqs. (18,21) [24–26]. The explicit form of the propagator is

$$G_R^{n+\frac{1}{2}} = \frac{P_{\mu_1\mu_2\dots\mu_n\nu_1\nu_2\dots\nu_n}^{n+\frac{1}{2}}}{p^2 - m_R^2 + im_R\Gamma_R}, \quad (\text{A1})$$

$$P_{\mu_1\mu_2\dots\mu_n\nu_1\nu_2\dots\nu_n}^{n+\frac{1}{2}} = \frac{n+1}{2n+3} (\not{p} + m) \gamma^\alpha \gamma^\beta P_{\alpha\mu_1\mu_2\dots\mu_n\beta\nu_1\nu_2\dots\nu_n}^{n+\frac{1}{2}}, \quad (\text{A2})$$

where

$$\begin{aligned} & P_{\mu_1\mu_2\dots\mu_n\nu_1\nu_2\dots\nu_n}^n \\ &= \left(\frac{1}{n!}\right)^2 \sum_{P_{[\mu_1]P_{[\nu_1]}}} \left[ \prod_{i=1}^n \tilde{g}_{\mu_i\nu_i} + a_1 \tilde{g}_{\mu_1\mu_2} \tilde{g}_{\nu_1\nu_2} \prod_{i=3}^n \tilde{g}_{\mu_i\nu_i} \right. \\ &+ \dots \\ &+ a_r \tilde{g}_{\mu_1\mu_2} \tilde{g}_{\nu_1\nu_2} \tilde{g}_{\mu_3\mu_4} \tilde{g}_{\nu_3\nu_4} \dots \tilde{g}_{\mu_{2r-1}\mu_{2r}} \tilde{g}_{\nu_{2r-1}\nu_{2r}} \prod_{i=2r+1}^n \tilde{g}_{\mu_i\nu_i} \\ &+ \dots \\ &\left. + \left\{ \begin{array}{l} a_{n/2} \tilde{g}_{\mu_1\mu_2} \tilde{g}_{\nu_1\nu_2} \dots \tilde{g}_{\mu_{n-1}\mu_n} \tilde{g}_{\nu_{n-1}\nu_n} \text{ (for even } n) \\ a_{(n-1)/2} \tilde{g}_{\mu_1\mu_2} \tilde{g}_{\nu_1\nu_2} \dots \tilde{g}_{\mu_{n-2}\mu_{n-1}} \tilde{g}_{\nu_{n-2}\nu_{n-1}} \tilde{g}_{\mu_n\nu_n} \text{ (for odd } n) \end{array} \right\} \right], \quad (\text{A3}) \end{aligned}$$

$$= \left(\frac{1}{n!}\right)^2 \sum_{P_{[\mu_1]P_{[\nu_1]}}} \sum_{r=0}^{[n/2]} a_r \prod_{i=1}^r \tilde{g}_{\mu_{2i-1}\mu_{2i}} \tilde{g}_{\nu_{2i-1}\nu_{2i}} \prod_{j=2r+1}^n \tilde{g}_{\mu_j\nu_j}, \quad (\text{A4})$$

with

$$a_{r(n)} = \frac{\left(-\frac{1}{2}\right)^r n!}{r!(n-2r)!(2n-1)(2n-3)\dots(2n-2r+1)}. \quad (\text{A5})$$

where  $\tilde{g}_{\mu\nu} = g_{\mu\nu} - \frac{q_\mu q_\nu}{q^2}$ ,  $P_{[\mu]}$  or  $P_{[\nu]}$  means the permutations for  $\mu$  or  $\nu$ , and  $[n]$  means integer round of  $n$ .

Some examples are presented in the followings:

$$G_R^{\frac{1}{2}} = \frac{(\not{p} + m)}{p^2 - m_R^2 + im_R\Gamma_R}, \quad (\text{A6})$$

$$G_R^{\frac{3}{2}} = G_R^{\frac{1}{2}} \left( -\tilde{g}_{\mu\nu} + \frac{1}{3} \tilde{\gamma}_\mu \tilde{\gamma}_\nu \right), \quad (\text{A7})$$

$$G_R^{\frac{5}{2}} = G_R^{\frac{1}{2}} \sum_{P_{[\mu]}, P_{[\nu]}}^2 \left[ \frac{1}{4} \tilde{g}_{\mu\nu} \tilde{g}_{\mu\nu} - \frac{1}{20} \tilde{g}_{\mu\mu} \tilde{g}_{\nu\nu} - \frac{1}{10} \tilde{\gamma}_\mu \tilde{\gamma}_\nu \tilde{g}_{\mu\nu} \right], \quad (\text{A8})$$

where  $\tilde{\gamma}_\nu = \gamma_\nu - \frac{p_\nu \not{p}}{p^2}$ .

### Appendix B: Extracting the coupling constants

As mentioned in section II B, the Lagrangians in Eqs. (18,21) show both radiative and strong decay of the nucleon resonance with  $J > 1/2$  are described by two coupling constants. In this appendix we will show how to extract coupling constants from the helicity amplitudes and partial decay amplitudes.

The helicity amplitudes for the resonances with spin-parity  $J^P$  can be calculated from the definition in Eq. (22) easily in the  $c.m.$  frame as

$$A_{\frac{1}{2}}(J^P) = \mathcal{P} \frac{ef_1}{2M_N} \sqrt{\frac{k_\gamma M_R}{M_N}}, \quad (\text{B1})$$

$$\begin{aligned} A_{\frac{3}{2}}(J^P) &= \mathcal{P} F_{\frac{3}{2}} k_\gamma^{n-1} \frac{e}{\sqrt{2}(2M_N)^n} \sqrt{\frac{k_\gamma M_R}{M_N}} \\ &\cdot \left[ f_1 + \left(\frac{\mathcal{P}}{M_R}\right) \frac{f_2}{4M_N} M_R(M_R + \mathcal{P}M_N) \right], \quad (\text{B2}) \end{aligned}$$

$$\begin{aligned} A_{\frac{1}{2}}(J^P) &= \mathcal{P} F_{\frac{1}{2}} k_\gamma^{n-1} \frac{e}{\sqrt{6}(2M_N)^n} \sqrt{\frac{k_\gamma M_N}{M_R}} \\ &\cdot \left[ f_1 + \frac{f_2}{4M_N^2} M_R(M_R + \mathcal{P}M_N) \right] \quad (\text{B3}) \end{aligned}$$

where  $F_r = \prod_{i=2}^n \langle 10, i - \frac{1}{2} r | i + \frac{1}{2} r \rangle$  and  $\mathcal{P} = P(-1)^n$  with  $n = J - \frac{1}{2}$ . Here  $M_N$  and  $M_R$  are the masses of nucleon and the nucleon resonance, and  $k_\gamma$  are the energy of the photon. The helicity amplitudes  $A_\lambda$  can be obtained by CQM or extracted from the experiment. Now the coupling constants for the resonances with  $J = \frac{1}{2}$  can be obtained from  $A_{1/2}$  directly and the ones with  $J > \frac{1}{2}$  can be solved from the two equations about  $A_{1/2}$  and  $A_{3/2}$ .

For the nucleon resonances decay to  $K$  and  $\Lambda^*(1520)$ , we have

$$\begin{aligned} \mathcal{A}(J^P, r, \theta) &= \langle K(\mathbf{q}) \Lambda^*(-\mathbf{q}, r) | -i \mathcal{H}_{\text{int}} | R(\mathbf{0}, r) \rangle \\ &= 4\pi M_R \sqrt{\frac{2}{q}} \sum_{\ell} \langle \ell 0 \frac{3}{2} r | J r \rangle Y_{\ell 0} G(\ell), \quad (\text{B4}) \end{aligned}$$

if we choose  $m_\ell = 0$ . Here  $\theta$  is the angle of the final  $K$ . The relative orbital angular momentum  $\ell$  of the final state is constrained by the spin-parity of the resonance. For the nucleon



resonances with  $J > 1/2$ , there are two  $\ell$  which is marked as  $\ell_1$  and  $\ell_2$  thereafter.

Since partial wave decay amplitudes  $G(\ell)$  is independent on the  $\theta$ , we choose  $\theta = 0$  and reach

$$A(J^P, \theta = 0, r) = \sqrt{\frac{2\ell_1 + 1}{4\pi}} \langle \ell_1 0 \frac{3}{2} r | J r \rangle G(\ell_1) + \sqrt{\frac{2\ell_2 + 1}{4\pi}} \langle \ell_2 0 \frac{3}{2} r | J r \rangle G(\ell_2) \quad (\text{B5})$$

The  $G(\ell)$  can be obtained from the CQM and is independent on  $r$ , so the difference of the amplitudes with different  $r$  is from the Clebsch-Gordan coefficient.

With certain  $J > \frac{1}{2}$  and  $r$ , the decay amplitudes can be calculated and has the form

$$A(J^P, r, \theta = 0)$$

$$= -\frac{\sqrt{8\pi M_R} q^{n-1}}{M_{\Lambda^*} m_K^n} \cdot \left[ h_1 \mathcal{P} [c_{l_0 \mathcal{P}} p^0 + (c_{1\mathcal{P}} - c_{l_0 \mathcal{P}}) M_{\Lambda^*}] \sqrt{p^0 + \mathcal{P} M_{\Lambda^*}} (M_R - \mathcal{P} M_{\Lambda^*}) + \frac{h_2}{m_K} M_R q^2 c_{l_0 \mathcal{P}} \sqrt{p^0 + \mathcal{P} M_{\Lambda^*}} \right] \quad (\text{B6})$$

where  $c_{1\pm}, l_{0\pm} = \prod_{i=2}^n \langle 10i - \frac{1}{2} r | i + \frac{1}{2} r \rangle [1, \delta_{l_0 0}] (|\langle 1l_0 \frac{1}{2} \frac{3}{2} r \rangle|^2 \pm |\langle 1l_0 \frac{1}{2} - \frac{3}{2} r \rangle|^2)$  and  $\mathcal{P} = P(-1)^{n+1}$ . Here  $M_{\Lambda^*}$  and  $m_K$  are masses of  $\Lambda(1520)$  and  $K$  meson, and  $p^0$  are the energy of the final  $\Lambda(1520)$ . Now the coupling constants  $h_1$  and  $h_2$  are related to the partial wave decay amplitudes  $G(\ell)$ . The  $h_1$  and  $h_2$  can be solved from above equations by choosing  $r = 1/2$  and  $r = 3/2$ .

- 
- [1] K. Nakamura et al. (Particle Data Group), J. Phys. G37, 075021 (2010) and 2011 partial update for the 2012 edition.
- [2] S. -H. Kim, S. -i. Nam, Y. Oh and H. -C. Kim, Phys. Rev. D **84**, 114023 (2011) [arXiv:1110.6515 [hep-ph]].
- [3] A. Kiswandhi and S. N. Yang, arXiv:1112.6105 [nucl-th].
- [4] J. F. Zhang, N. C. Mukhopadhyay and M. Benmerrouche, Phys. Rev. C **52**, 1134 (1995) [hep-ph/9506238].
- [5] K. Nakayama and H. Haberzettl, Phys. Rev. C **73**, 045211 (2006) [nucl-th/0507044].
- [6] X. -H. Zhong and Q. Zhao, Phys. Rev. C **84**, 065204 (2011) [arXiv:1110.5466 [nucl-th]].
- [7] J. He, B. Saghai Phys. Rev. C **80**, 015207 (2009) [arXiv:0812.1617 [nucl-th]].
- [8] A. Boyarski, R. E. Diebold, S. D. Ecklund, G. E. Fischer, Y. Murata, B. Richter and M. Sands, Phys. Lett. B **34**, 547 (1971).
- [9] D. P. Barber *et al.*, Z. Phys. C **7**, 17 (1980).
- [10] T. Nakano *et al.* [LEPS Collaboration], Phys. Rev. Lett. **91**, 012002 (2003) [arXiv:hep-ex/0301020].
- [11] N. Muramatsu *et al.*, Phys. Rev. Lett. **103**, 012001 (2009) [arXiv:0904.2034 [nucl-ex]].
- [12] S. I. Nam and C. W. Kao, Phys. Rev. C **81**, 055206 (2010) [arXiv:1003.0700 [hep-ph]].
- [13] H. Kohri *et al.* [LEPS Collaboration], Phys. Rev. Lett. **104**, 172001 (2010) [arXiv:0906.0197 [hep-ex]].
- [14] J. J. Xie and J. Nieves, Phys. Rev. C **82**, 045205 (2010) [arXiv:1007.3141 [nucl-th]].
- [15] S. Capstick and W. Roberts, Phys. Rev. D **58**, 074011 (1998) [nucl-th/9804070].
- [16] S. Capstick, Phys. Rev. D **46**, 2864 (1992).
- [17] Y. Oh, C. M. Ko, K. Nakayama, Phys. Rev. **C77**, 045204 (2008). [arXiv:0712.4285 [nucl-th]].
- [18] S. I. Nam, A. Hosaka and H. C. Kim, Phys. Rev. D **71**, 114012 (2005) [arXiv:hep-ph/0503149].
- [19] H. Toki, C. Garcia-Recio and J. Nieves, Phys. Rev. D **77**, 034001 (2008) [arXiv:0711.3536 [hep-ph]].
- [20] T. Hyodo, S. Sarkar, A. Hosaka and E. Oset, Phys. Rev. C **73**, 035209 (2006) [Erratum-ibid. C **75**, 029901 (2007)] [arXiv:hep-ph/0601026].
- [21] A. I. Titov, B. Kampfer, S. Date and Y. Ohashi, Phys. Rev. C **72**, 035206 (2005) [Erratum-ibid. C **72**, 049901 (2005)] [arXiv:nucl-th/0506072].
- [22] M. Guidal, J. M. Laget and M. Vanderhaeghen, Nucl. Phys. A **627**, 645 (1997).
- [23] T. Corthals, T. Van Cauteren, J. Ryckebusch and D. G. Ireland, Phys. Rev. C **75**, 045204 (2007) [arXiv:nucl-th/0612085].
- [24] S. -J. Chang, Phys. Rev. **161**, 1308 (1967).
- [25] J. G. Rushbrooke, Phys. Rev. **143**, 1345 (1966).
- [26] R. E. Behrends and C. Fronsdal Phys. Rev. **106**, 345 (1957).
- [27] J. J. Wu, Z. Ouyang and B. S. Zou, Phys. Rev. C **80**, 045211 (2009) [arXiv:0902.2295 [hep-ph]].
- [28] Zhiwen Zhao, Presented at the 8th Workshop on the Physics of Excited Nucleons (NSTAR2011), Newport News, USA, May 2011
- [29] F. W. Wieland, *et al.*, arXiv:1011.0822 [nucl-ex].